Self-consistent GW_0 results for the electron gas: Fixed screened potential W_0 within the random-phase approximation

Ulf von Barth and Bengt Holm
Department of Theoretical Physics, University of Lund, Sweden
(Received 29 April 1995)

With the aim of properly understanding the basis for and the utility of many-body perturbation theory as applied to extended metallic systems, we have calculated the electronic self-energy of the homogeneous electron gas within the GW approximation. The calculation has been carried out in a self-consistent way; i.e., the one-electron Green function obtained from Dyson's equation is the same as that used to calculate the self-energy. The self-consistency is restricted in the sense that the screened interaction W is kept fixed and equal to that of the random-phase approximation for the gas. We have found that the final results are marginally affected by the broadening of the quasiparticles, and that their self-consistent energies are still close to their free-electron counterparts as they are in non-self-consistent calculations. The reduction in strength of the quasiparticles and the development of satellite structure (plasmons) gives, however, a markedly smaller dynamical self-energy leading to, e.g., a smaller reduction in the quasiparticle strength as compared to non-self-consistent results. The relatively bad description of plasmon structure within the non-self-consistent GW approximation is marginally improved. A first attempt at including W in the self-consistency cycle leads to an even broader and structureless satellite spectrum in disagreement with experiment. [S0163-1829(96)05136-3]

I. INTRODUCTION

In the late 1950s the techniques of field theory and many-body perturbation theory (MBPT) were incorporated into the tool box of solid-state theory. After an enthusiastic period in the beginning of the 1960s, when a lot of fundamental theorems were proven and some numerical results were obtained for a few systems, especially for the electron gas, the activity within this area of research showed a marked decline. This was certainly not caused by a widespread feeling that most important problems were already solved, although remarks to that effect can nowadays be found in the literature. Instead there were two obvious reasons for the diminishing interest in many-body perturbation theory as applied to real solids. The numerical difficulties associated with evaluating anything but the most simpleminded approximations in real solids were prohibitively large. Second, the original enthusiasm was damped by the realization that, at least in highly degenerate metallic systems, one is dealing with a divergent perturbation series. Thus the choice of physical processes or diagrams to include in a particular approximation must be guided by physical insight and intuition. There is thus no systematic way of obtaining successively better approximations.

Armed with modern computers and with a better knowledge on how to describe the underlying one-electron structure in a very efficient way, we are now able to apply more complicated and therefore more realistic approximations within MBPT to real solids. These efforts are exemplified by the so called GW calculations for different semi-conductors,[1–3] and for the transition metals[4–6] and their oxides.[7]

The GW approximation[8] owes its name to the fact that it is defined by approximating the electronic self-energy as a product of the Green function G and the screened interaction W. In this way one obtains one of the simplest possible extensions of Hartree-Fock theory by replacing the bare Coulomb interaction by a dynamically screened interaction (W). Thus the GW approximation could equally well have been referred to as the dynamically screened exchange approximation. The GW approximation has a number of desirable physical properties in most physical systems ranging from atoms to the electron gas. For a review of these we refer to Ref. 9. For one thing, the GW approximation gives a very accurate description of the quasiparticles in all systems to which it has been applied. It is important to stress, however, that these nice features are not consequences of the GW approximation being the lowest-order correction in a rapidly convergent perturbation expansion starting from the independent-particle approximation. On the contrary, it has proven exceedingly difficult to go beyond the GW approximation, and results most often deteriorate by adding higher-order corrections.

In the original formulation of the GW approximation,[8] the Green function used to generate the electronic self-energy within the GW approximation, was the Green function obtained from Dyson's equation in which the same self-energy appeared as a nonlocal energy dependent potential. The self-consistency implied by this prescription has never been attempted in any realistic system — not even in the electron gas. As far as we know, the first fully self-consistent GW calculation was recently carried out for a model system consisting of a quasi-one-dimensional semiconducting wire.[10] Unfortunately, the relevance of this model to actual solids is somewhat unclear.[10] Nevertheless, it was shown early on[11,12] that such a self-consistent scheme results in a so-called conserving approximation which automatically obeys several sum rules and consistency requirements like, e.g., particle conservation and energy conservation under the influence of external perturbations. Moreover, it has been demonstrated, e.g., in NiO,[7] that the effect of self-consistency can be large

in strongly correlated systems and possibly also in systems with weaker correlation effects.

Comparing the starting Green function — usually chosen to be that obtained from a self-consistent local-density (LD) calculation — with the Green function obtained after one iteration toward self-consistency (i.e., what has been achieved so far in solids), one can distinguish four major effects of self-consistency. (i) The quasiparticles are broadened, indicating their finite lifetime. (ii) The quasiparticle energies are shifted. (iii) The strength of the quasi-particle peak is significantly reduced (typically by one third), and the spectral weight is transferred to different system dependent satellite structures. (iv) The average screening properties of the medium is altered due to an interacting Green function appearing in the dynamically screened interaction (W). It is not difficult to realize that a marked reduction in quasiparticle weight could easily lead to a significantly smaller self-energy. In this way, the nice agreement obtained between theory and experiment for, e.g., the band gaps of semiconductors or the band widths of transition metals could be destroyed by self-consistency.

Being interested in understanding many-body perturbation theory and in its usefulness with regard to physical properties, we believe it is important to pursue the issue of self-consistency. Our ultimate aim is a study of the effects of self-consistency in strongly correlated systems. In view of the extent of such a project and because of the numerical difficulties associated with it, we decided to gain some preliminary insight through numerical calculations for the electron gas. In this way, we could study the four separate effects discussed above. Our preliminary results indicate that the largest effect of self-consistency is associated with a modification of the screening effects. Instead of distinct plasmon satellites, the results show a broad structureless satellite spectrum, in clear contradiction with experimental data. These results suggest that non-self-consistent self-energies are to be preferred. Before pursuing full self-consistency any further, we decided, however, to carry out a restricted self-consistency, keeping the screened interaction fixed in the process. Such a limited self-consistency is what presently might be within our computational feasibility in realistic systems. The converged results of this paper are thus obtained by, as our fixed $W=W_0$, using that of the random-phase approximation (RPA) based on the noninteracting Green function. In this way, we can study the three effects (i)–(iii) discussed above, but not the fourth effect. This will be postponed until a later publication.

In Sec. II we recapitulate some basic results of MBPT, and present those basic ideas which make self-consistent GW calculations a relatively straightforward procedure, at least for the electron gas. In Sec. III we present a useful sum rule valid within all GW-type procedures, and discuss some numerical details. Our results are discussed in Sec. IV, and our conclusions are summarized in Sec. VI. Some preliminary results of forthcoming work on including the screening effects in the self-consistency procedure are discussed in Sec. V.

II. THEORY AND BASIC PROCEDURES

In performing a self-consistent calculation for the electronic self-energy or, which amounts to the same thing, for the one-electron Green function G, one must evidently save some representation of, i.e., G from one iteration to the next. This is assuming the self-consistency problem can be solved by an iterative procedure, which actually turns out to be the case. As a minimal and convenient representation for G we have chosen its spectral function A, which completely determines G through the Lehmann representation

$$G(\mathbf{k},\omega)=\int_C \frac{A(\mathbf{k},\omega')}{\omega-\omega'}d\omega', \tag{1}$$

where C is the contour in the complex frequency plane defined as a straight line from $-\infty$ to 0 just above the real axis and another straight line from 0 to ∞ just below the real axis. At this point we mention that here and throughout this paper, the zero of energy is always chosen at the Fermi energy. Thus all propagators, fermion or boson, interacting or noninteracting, always change their analytic structure at $\omega=0$.

We also note that, due to the full translational and rotational symmetry of the homogeneous gas, the spectral function $A(\mathbf{k},\omega)$ is diagonal in reciprocal space ($\mathbf{k}$ space) and depends only on the absolute magnitude k of $\mathbf{k}$. These two features simplify the calculations in a decisive way.

Instead of representing the function A as a numerical matrix in k and ω, we have chosen a representation in terms of Gaussian basis functions:

$$A(k,\omega)=\sum_\nu \frac{W_\nu(k)}{\sqrt{2\pi}\Gamma_\nu(k)}\exp\left[-\frac{[\omega-E_\nu(k)]^2}{2\Gamma_\nu^2(k)}\right]. \tag{2}$$

Here, the quantities $E_\nu(k)$, $\Gamma_\nu(k)$, and $W_\nu(k)$ are numerical functions of k which, in actual fact, also are easily parametrized in terms of relatively simple analytical formulas which we, however, refrain from presenting here.

The representation defined by Eq. (2) has several advantages. First of all, any positive definite spectral function A can be represented in this way to any desired degree of accuracy. More importantly, already with very few terms in the sum over ν, the representation has the form one expects for the A of an interacting system. A main quasiparticle peak with a certain energy position and a certain broadening plus a few sidebands corresponding to plasmon satellites are easily modeled by Eq. (2). The actual form of the different peaks is easily accounted for by adding a few more Gaussians. It should be kept in mind that the output for $A(k,\omega)$ from one iteration is completely numerical. These numerical results are then fitted to the form given by Eq. (2), which, in turn, is used as input for the next iteration. It turns out that, when approaching self-consistency, the details of the shape of the input A have a very small effect on the output A as long as the main physical effects are correctly described. This means, e.g., that the output A is very insensitive to the detailed shape of the plasmon satellites as long as their weights and positions are correct, and the same is true for the dominant quasiparticle peak. Numerically, we have found that, e.g., quasiparticle energies or renormalization factors are converged to within two significant digits using only three terms in Eq. (2). For the final converged results, we have used five terms in Eq. (2).

Let us now go to a description of the screened interaction $W_0(\mathbf{q},\omega)$, which, in the present work, is obtained from the

RPA and thus simply related to the bare Coulomb interaction $v(q)=4\pi/q^2$ and the frequency-dependent Lindhart function $\chi_0(q,\omega)$ (see Ref. 9) (again due to symmetry, W is a function only of the magnitude q of $\mathbf{q}$),

$$W_0(q,\omega)=v(q)+v(q)\chi_0(q,\omega)W_0(q,\omega). \tag{3}$$

In order to facilitate the calculations we also need the spectral function $B(q,\omega)$ of W defined in the usual way [see Eq. (1)],

$$W_0(q,\omega)=v(q)+\int_C \frac{B_0(q,\omega')}{\omega-\omega'}d\omega', \tag{4}$$

where

$$B_0(q,\omega)=-\frac{1}{\pi}\frac{v^2(q)\ \mathrm{Im}\chi_0(q,\omega\ )}{|\ 1\ -\ v(q)\chi_0(q,\omega\ )\ |^2}\mathrm{sgn}(\omega). \tag{5}$$

The real and imaginary parts of $\chi_0(q,\omega)$ are simple analytical expressions in q and ω which, however, we refrain from giving here.

We now remind the reader that the *GW* approximation is defined[8] by the following approximation for the self-energy $\Sigma(\mathbf{k},\omega)$:

$$\Sigma(\mathbf{k},\omega)=i\sum_{\mathbf{q}}\ \int\frac{d\omega'}{2\pi}G(\mathbf{k}+\mathbf{q},\omega+\omega')W_0(\mathbf{q},\omega'), \tag{6}$$

where $\Sigma_{\mathbf{q}}$ is short for $(2\pi)^{-3}\int d^3q$. It is well known [it follows directly from Eq. (6)] that the self-energy of the *GW* approximation has the correct analytic properties of a fermion propagator, and consequently has a Lehmann representation of the form

$$\Sigma(\mathbf{k},\omega)=\Sigma_{\mathrm{HF}}(\mathbf{k})+\int_C\frac{\Gamma(\mathbf{k},\omega')}{\omega-\omega'}d\omega' \tag{7}$$

in terms of a positive definite spectral function $\Gamma(\mathbf{k},\omega)$. The high-frequency limit $\Sigma_{\mathrm{HF}}(\mathbf{k})$ of Σ is the energy-independent Hartree-Fock part of the self-energy given by the usual expression

$$\Sigma_{\mathrm{HF}}(\mathbf{k})=-\sum_{\mathbf{q}}\ v(\mathbf{k}+\mathbf{q})n_{\mathbf{q}}, \tag{8}$$

where, however, the momentum distribution $n_{\mathbf{k}}$ is that of the interacting gas within this approximation. Thus,

$$n_{\mathbf{k}}=\int_{-\infty}^{0}A(\mathbf{k},\omega)d\omega. \tag{9}$$

Combining the three spectral representations, Eqs. (1), (4), and (7), with the definition, Eq. (6), of the *GW* approximation we obtain the following relation between the three spectral functions A, B_0, and Γ:

$$\Gamma(\mathbf{k},\omega)=\sum_{\mathbf{q}}\ \int_0^{\omega}A(\mathbf{k}+\mathbf{q},\omega-\omega')B_0(\mathbf{q},\omega')d\omega'. \tag{10}$$

Since B_0 remains fixed during the calculation, a knowledge of A suffices to determine Γ and therefore Σ through Eq. (7). In order to close the self-consistency cycle we need to connect Σ to A or, equivalently, to G, and for this purpose we have Dyson's equation

$$G(\mathbf{k},\omega)=G_0(\mathbf{k},\omega)+G_0(\mathbf{k},\omega)\Sigma(\mathbf{k},\omega)G(\mathbf{k},\omega). \tag{11}$$

Here the free-electron Green function $G_0(\mathbf{k},\omega)$ is simply given by

$$G_0(k,\omega)=\frac{1}{\omega-\epsilon_k}, \tag{12}$$

with ϵ_k being equal to $k^2/2$. We note in passing that Dyson's equation results from an infinite partial summation of Feynman graphs.

At this point we remind the reader that, in the present work, we consider shifted correlation functions where $\omega=0$ corresponds to the Fermi energy μ. Thus, $\epsilon_k=k^2/2$ in Eq. (12) needs to be shifted to $\epsilon_k=k^2/2-\mu$. Now, by definition, μ is the position of the pole of the Green function at the Fermi momentum k_F and, consequently, from Dyson's equation above:

$$\mu=\epsilon_F+\tilde{\Sigma}(k_F,\mu). \tag{13}$$

Here $\tilde{\Sigma}(\omega)$ represents the ''normal'' unshifted self-energy, i.e., $\tilde{\Sigma}(\omega)=\Sigma(\omega-\mu)$ in terms of our shifted self-energy Σ. The Fermi momentum k_F is given by the usual expression $k_F=(3\pi^2n)^{1/3}$, n being the density of the gas, and ϵ_F the Fermi energy of free electrons, i.e., $\epsilon_F=k_F^2/2$. Thus, in total, ϵ_k in Eq. (12) should be

$$\epsilon_k=\tfrac{1}{2}k^2-\tfrac{1}{2}k_F^2-\Sigma(k_F,0). \tag{14}$$

Finally, using the Lehman representation for the Green function, Eq. (1), and for the self-energy, Eq. (7), and taking imaginary parts of both sides of Dyson's equation, Eq. (11), we arrive at

$$A(k,\omega)=\frac{\Gamma(k,\omega)}{|\omega-\epsilon_k-\Sigma(k,\omega)|^2}. \tag{15}$$

This is the desired relation that closes our self-consistency cycle.

Using the formulas presented above, our calculational procedure is easily described as follows. We start from some guessed representation of A in terms of Eq. (2). In order to make contact with previous work on the electron gas,[13–16] we usually start with a noninteracting A given by G_0 of Eq. (12). For each k, we then obtain Γ from Eq. (10), and subsequently A from Eq. (15). This purely numerical result for A is then refitted to the form in Eq. (2), and the procedure is repeated until no further changes occur in the output A.

III. SUM RULE AND NUMERICS

In this section we will derive a useful sum rule which we have not seen earlier in the literature, and which is generally valid within the *GW* approximation whether self-consistent or not. We will also give some details concerning our numerical procedures, and describe a more accurate way of obtaining the momentum distribution function $n_{\mathbf{k}}$, defined in Eq. (9).

Due to the well-known sum rule (see, e.g., Ref. 9)

$$\int_{-\infty}^{\infty}A(\mathbf{k},\omega)d\omega=1, \tag{16}$$

the high-frequency limit of $G(\omega)$ is always $1/\omega$. Thus by taking the high-frequency limits of Eqs. (6) and (7) and equating the coefficients of $1/\omega$, we obtain

$$\int_{-\infty}^{\infty}\Gamma(\mathbf{k},\omega)d\omega=\sum_{\mathbf{q}}\int_{0}^{\infty}B_0(\mathbf{q},\omega)d\omega, \tag{17}$$

where we have also used the spectral representation [Eq. (4)] of W_0. There are two noteworthy features to this sum rule. (i) This particular integral over Γ, which, in turn, determines the self-energy, is independent of self-consistency and is only a consequence of the prechosen screened potential W_0. This means that, although a reduction of the strength of the quasiparticle will give a smaller dynamical self-energy at some energies, mainly at the quasiparticle energy, the total spectral weight of the self-energy is conserved. (ii) The left-hand side of Eq. (17) is $\mathbf{k}$ dependent, but the right-hand side is not. Thus the total spectral density of the self-energy does not vary with the $\mathbf{k}$ vector of the excitation. In our calculation we have found it convenient to use the derived sum rule as a check on our numerical accuracy. Two other sum rules which are also useful for numerical purposes are readily obtained from the high-frequency limits of Eqs. (1), (7), and (11):

$$\int_{-\infty}^{\infty}\omega A(\mathbf{k},\omega)d\omega=E_{\mathbf{k}}^{\mathrm{HF}}, \tag{18}$$

$$\int_{-\infty}^{\infty}\omega^2 A(\mathbf{k},\omega)d\omega=\int_{-\infty}^{\infty}\Gamma(\mathbf{k},\omega)d\omega+(E_{\mathbf{k}}^{\mathrm{HF}})^2, \tag{19}$$

where

$$E_{\mathbf{k}}^{\mathrm{HF}}=\epsilon_{\mathbf{k}}+\Sigma_{\mathrm{HF}}(\mathbf{k}) \tag{20}$$

is the quasiparticle energy in the Hartree-Fock approximation [although obtained from an interacting momentum distribution, cf. Eq. (9)].

Due to the very sharp quasiparticle structure in $A(k,\omega)$, it is numerically difficult to obtain the momentum distribution $n_{\mathbf{k}}$ directly from the definition [Eq. (9)]. An accurate value for $n_{\mathbf{k}}$ is needed, e.g., in order to check whether particle conservation is obeyed at least approximately in this calculation with restricted self-consistency. We would thus like to check if

$$2\sum_{\mathbf{k}} n_{\mathbf{k}}=n, \tag{21}$$

where the 2 comes from the spin degeneracy. For this purpose, we first write

$$A(\mathbf{k},\omega)=-\frac{1}{\pi}\,\mathrm{Im}\,G(\mathbf{k},\omega)\mathrm{sgn}(\omega), \tag{22}$$

and then observe that, for $\omega<0$, $G(\omega)$ is the limit when $\mathrm{Im}\omega\to 0^-$ of a function which is analytic in the lower half-plane. This allows us to deform the frequency integral along the negative real axis to the negative imaginary axis, thereby picking up a contribution from the quarter circle. We obtain

$$n_{\mathbf{k}}=\tfrac{1}{2}+\frac{1}{\pi}\,\mathrm{Re}\int_{0}^{\infty}G(\mathbf{k},-i\omega)d\omega \tag{23}$$

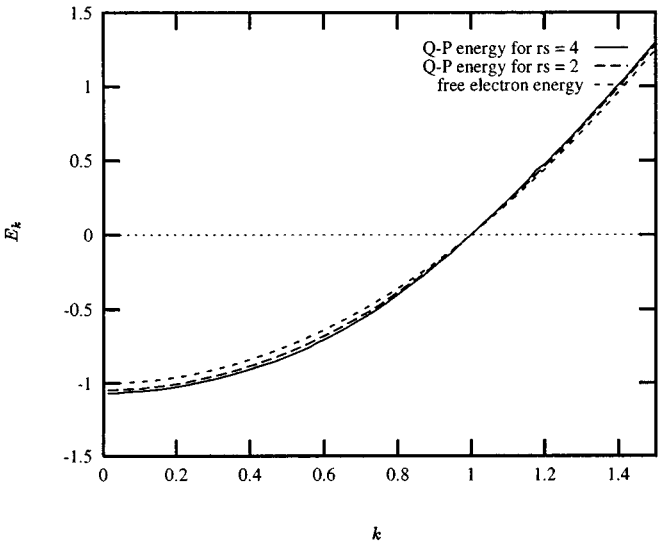

FIG. 1. The quasiparticle renormalization factor $Z(k)$ as a function of momentum $k(r_s=4)$.

and for $G(\mathbf{k},\omega)$ we use Dyson's equation [Eq. (11)] in which all quantities including Σ are smooth and well behaved at the negative imaginary axis.

The quasiparticle energies $E_{\mathbf{k}}$ are the energy positions of well-defined peaks in the spectral function $A(\omega)$. From Eq. (15) we see that they are given by the solutions of the quasiparticle equation

$$E_{\mathbf{k}}=\epsilon_{\mathbf{k}}+\mathrm{Re}\Sigma\,(\mathbf{k},E_{\mathbf{k}}). \tag{24}$$

If the imaginary part of Σ becomes large, signaling more ill-defined quasiparticles, there could be a small deviation between the $E_{\mathbf{k}}$ as defined by Eq. (24) and the actual position of the maximum of the peak. In this work, we have not had reason to consider this case. In fact, the imaginary part of Σ is small throughout the band, and quasiparticle energies are close to the free-electron energies ($k^2/2-k_F^2/2$; see Fig. 3). This fact immediately suggests a fast way of obtaining a solution to the nonlinear quasiparticle equation. Expanding $\mathrm{Re}\,\Sigma$ around $\epsilon_{\mathbf{k}}+\Delta$, where $\Delta=\Sigma(k_F,0)$, to first order in the difference between the quasiparticle and the free-electron energies gives

$$E_k=\epsilon_k+\Delta+Z(k)[\Sigma(k,\epsilon_k+\Delta)-\Delta], \tag{25}$$

where

$$Z(k)=\left[1-\frac{\partial\,\mathrm{Re}\Sigma\,(k,\epsilon_k+\Delta\,)}{\partial\,\omega}\right]^{-1} \tag{26}$$

is the quasiparticle renormalization factor. We have found this linear approximation to be accurate enough for our purposes, i.e., for the plots in the figures.

The quasiparticle renormalization factor $Z(k)$ is seen (Fig. 1) to be relatively constant over the occupied part of the band and at the Fermi surface $Z_F=Z(k_F)$, we take it as a measure of the correlation effects (also see Table I). When the quasiparticle is reduced in strength (scaled down by Z_F) we expect the self-energy to be similarly reduced in magnitude, although maybe not to the same extent since some contributions to Σ come from the incoherent part of the

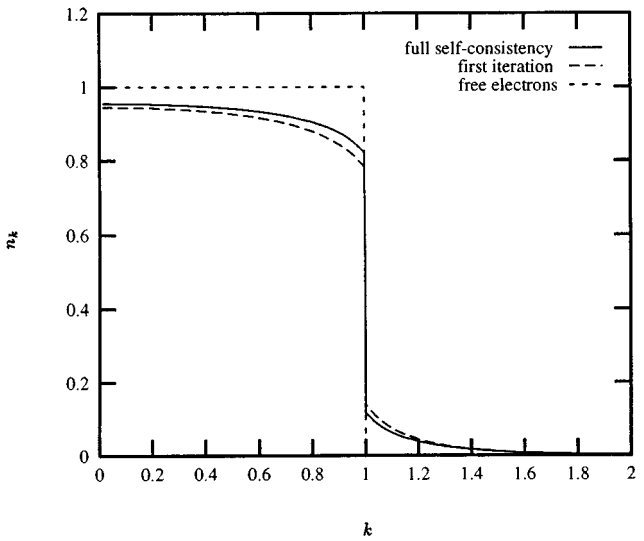

FIG. 2. The self-consistent spectral function $A(k=k_F,\omega)$ [Eq. (1)] is shown at two different levels of approximations using three and five Gaussians in Eq. (1). This demonstrates the insensitivity of the output $A(\omega)$ to the input $A(\omega)$.

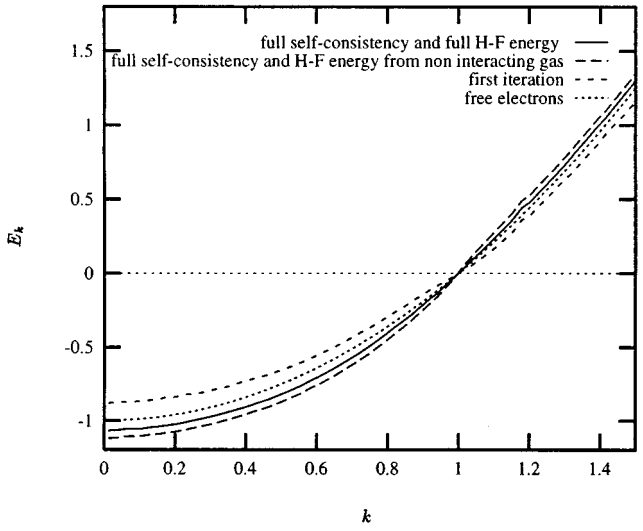

FIG. 3. The self-consistent spectral function of the self-energy at the Fermi surface $(k/k_F=1)$ compared to that of the first iteration. Note the reduction in magnitude and the spreading of the total weight.

Green function, a part which is enhanced rather than diminished. Let us simply assume $\partial\Sigma/\partial\omega$ to be proportional to Z_F allowing us to write [see Eq. (26)]

$$Z_F=\frac{1}{1+\gamma Z_F}, \tag{27}$$

with some constant of proportionality γ. At the first iteration, we start with free particles $(Z=1)$ and obtain a renormalization factor Z_1. Thus

$$Z_1=\frac{1}{1+\gamma}. \tag{28}$$

Eliminating γ between Eqs. (27) and (28) gives

$$Z_F=\frac{2}{\sqrt{4/Z_1-3}+1}, \tag{29}$$

a formula that actually allows us to obtain the fully self-consistent renormalization factor Z_F from a knowledge of that of the first iteration. We have found numerically that this formula [Eq. (29)] is quite accurate, and it can be used to speed up convergence.

The heaviest part, or rather the least easy part, of the calculations are associated with obtaining the spectral function Γ from Eq. (10). Due to spherical symmetry the convolution integral in **k** space involves only the azimuthal angle which is converted to a momentum integral. Thus Eq. (10) amounts to a double integral in **k** space and a single integral over the frequency. For the momentum integrals we have used altogether 168 points from zero to $4k_F$, and for the frequency integrals we have used altogether 558 points from $-8E_F$ to $16E_F$.

As discussed in Sec. II, the output spectral function $A(\omega)$ depends weakly on the details in the input $A(\omega)$, as long as the latter has the correct physical content, i.e., correct quasiparticle weight, position and broadening, and approximately the correct satellite positions. In fact, using only three Gaussians in Eq. (2), i.e., one for the quasiparticle peak and one each for the first high- and low-energy plasmon satellites, gives almost self-consistent results. This can be seen in Fig. 2, comparing output $A(\omega)$'s from using three and five Gaussians.

In all this work momenta are in units of the Fermi momentum (k_F) and all energies in units of the Fermi energy $(k_F^2/2)$. As is evident from many formulas, the chemical potential is chosen to be the zero of energy.

TABLE I. Quasiparticle renormalization factor at the Fermi surface Z_F [Eq. (25)] at two different densities for the self-consistent (SC) result and for the first (1st) iteration. SC3 and SC5 are results using three and five Gaussians in Eq. (2) thus demonstrating the usefulness of the Gaussian representation.

	Z_F		
r_s	1st	SC3	SC5
2	0.764	0.804	0.807
4	0.645	0.702	0.706

IV. RESULTS

We have chosen to present most of our results in the form of several figures. Since our model (the electron gas) is not directly applicable to any real system, we are mainly interested in the qualitative effects of self-consistency and not so much in the precise numbers.

In Fig. 3 we display the self-consistent spectral function $\Gamma(k_F,\omega)$ of the self-energy. It is compared with the corresponding quantity from the first iteration starting from non-interacting electrons, and we see the main effects of self-consistency. The spectral function Γ is reduced in magnitude, and the oscillator strength is shifted away from the Fermi level in order to preserve the total weight in accordance with the sum rule [Eq. (17)]. This reduced spectral

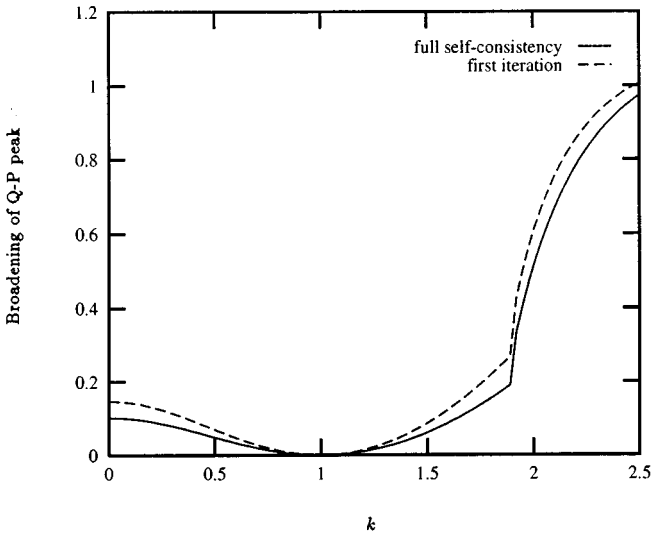

FIG. 4. The real part of the self-energy of the self-consistent calculation and of the first iteration, respectively. Note the less steep slope at the Fermi energy for the self-consistent case.

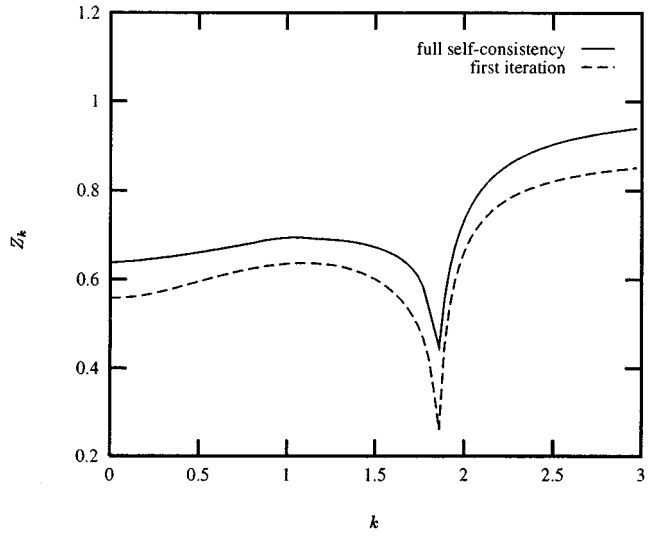

FIG. 5. The quasiparticle dispersion ($E_{\mathbf{k}}$) for two electron densities $r_s=2$ and 4, where r_s is the usual electron-gas parameter. The largest change in the bandwidth occurs for $r_s=4$.

function will of course produce a smaller dynamical self-energy [Eq. (7)], as can be seen in Fig. 4. [By the dynamical self-energy we mean that part of the self-energy which is due to correlations and which tends to zero at large ω; see Eq. (7).] The slope of the real part of the self-energy at the quasiparticle energy is a measure of the renormalization factor. The smaller slope of the self-consistent result leads to a larger renormalization factor (Z_F), and a smaller reduction of the strength of the quasiparticle as compared to the results of the first iteration [Eq. (26)].

In Fig. 5 we give the dispersion of the quasiparticle energies $E_{\mathbf{k}}$ for two different densities of the gas corresponding to $r_s=2$ and 4, where r_s is the usual radius of a sphere corresponding to the volume per electron. It is seen that the high-density result is indeed very close to the free-electron dispersion. At lower density ($r_s=4$) the correlation effects are more pronounced, and for this reason most of our fully self-consistent results are shown at that density.

In Fig. 6 we compare the self-consistent momentum distribution function $n_{\mathbf{k}}$ with those of the first iteration, and of noninteracting electrons at $r_s=4$. Note that the discontinuity at the Fermi surface is again the quasiparticle renormalization factor Z_F which, however, now is obtained from Eq. (23) rather than from Eq. (26). We take the near equality between the values obtained from these two very different methods as a consistency check on our calculations. Figure 6 shows again the increase in quasiparticle strength caused by self-consistency.

Provided the present approximation with a restricted self-consistency is particle conserving, the momentum distribution function can be integrated to yield the particle density [see Eq. (26)]. This has been done numerically, and we have found the present scheme to be particle conserving to within the accuracy of the calculation (four digits for n). It should also be possible to investigate this point analytically, although we have so far made no attempt in this direction.

The quasiparticle dispersion $E_{\mathbf{k}}$ is again shown in Fig. 7, but this time compared with the corresponding results from the first iteration. In the first iteration one obtains a promising band narrowing which, however, is too small compared to experiment[17] in sodium, with an electron density corresponding to $r_s=4$. Unfortunately, the self-consistency destroys this nice feature and gives a band wider than the free-electron result, in clear contradiction to experiment.[17] This clearly indicates the necessity for vertex corrections. The results would have been even worse if it were not for the fact that the Hartree-Fock contribution to the dispersion is also reduced because of the interacting momentum distribution function appearing in Eq. (8). The results can be understood as follows. The Hartree-Fock self-energy contribution widens the gap by a large factor, but the dynamical part [the last term in Eq. (7)] of Σ almost cancels this effect in the first

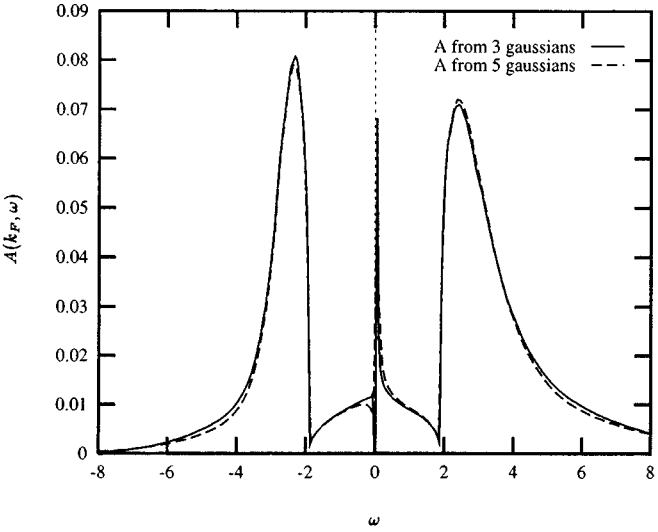

FIG. 6. The momentum distribution function $n_{\mathbf{k}}$ of the electrons for three cases: (i) the self-consistent case, (ii) the first iteration, and (iii) the noninteracting electron gas. The quasiparticle renormalization factor at the Fermi surface here shows up as the magnitude of the discontinuity, which is increased by self-consistency ($r_s=4$).

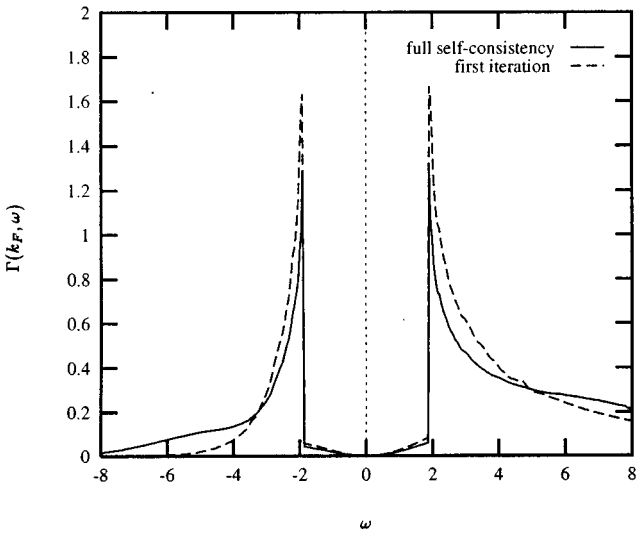

FIG. 7. The self-consistent quasiparticle dispersion compared to that from the first iteration. Also shown is the free-electron dispersion and that obtained by using the noninteracting $n_{\mathbf{k}}$ when calculating the Hartree-Fock self-energy ($r_s=4$).

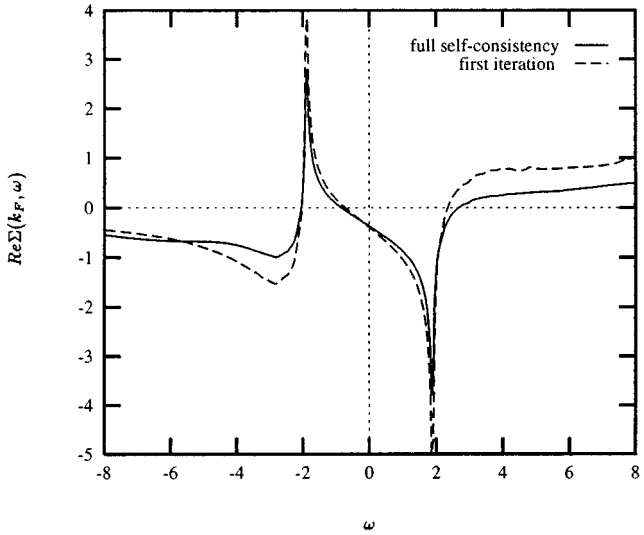

FIG. 8. The broadening of the quasiparticle peak as obtained from the spectral function (multiplied by π) of the self-energy evaluated at the quasiparticle energy. The sharpening of the quasiparticle peak due to self-consistency is evident ($r_s=4$).

iteration, and we obtain a very free-electron-like behavior. When we go to self-consistency, the reduction in strength of the quasiparticle causes a smaller dynamical part of the self-energy, which is no longer large enough to cancel the very large exchange part. The fact that the latter is also somewhat reduced by self-consistency cannot alter this fact, and we obtain too large a bandwidth.

Self-consistency also has an important effect on the quasiparticle broadening which, in turn, has a negligible effect on the outcome of the calculation. This leads, however, to sharper quasiparticles especially closer to the band bottom (see Fig. 8), an effect which should be possible to observe experimentally.

In Figs. 9 to 11, we show the spectral function $A(\omega)$ with its satellite structure, and compare the full results with those of the first iteration. We see that the bad description of the plasmon satellite that we are used to from ordinary GW calculations (first iteration) is not much improved by self-consistency. Although the plasmon peak becomes sharper and moves closer to the main peak, it is still too diffuse and too far away from the main peak — especially away from the Fermi surface. This discouraging result is not going to be remedied by including the screened interaction W in the self-consistency (see below), and again clearly indicates the need for including vertex corrections.

V. SELF-CONSISTENT SCREENING

As discussed above, we also intend to include the screened interaction $W(\mathbf{q},\omega)$ in the self-consistency, as was advocated by Kadanoff and Baym[11,12] in order to have a conserving approximation. The full results of such work will be postponed to a forthcoming publication. We will here just indicate those results of that work that can be obtained from simple reasoning. When the self-consistent Green function is used also for obtaining W through the GG polarization diagram, the spectral function $B_0(\mathbf{q},\omega)$ of W becomes[18]

$$S_0(\mathbf{q},\omega)=2\sum_{\mathbf{k}}\int_0^{\omega}A(\mathbf{k},\omega'-\omega)A(\mathbf{k}+\mathbf{q},\omega')d\omega'. \quad (30)$$

This function $S_0(\omega)$ is the spectral function which replaces that of the normal Lindhart function χ_0, and from which we obtain the spectral function $B(\mathbf{q},\omega)$ of $W(\mathbf{q},\omega)$ by solving Eq. (3). It can then be seen that, when $A(\omega)$ develops a sharp plasmon structure at the energy ω_p below the quasiparticle peak, then $S_0(\omega)$, being the convolution of two A's, will have peaks at ω_p and $2\omega_p$ above zero. Consequently, the spectral function $B(\omega)$ will be suppressed around $\omega=\omega_p$, resulting in a disappearance of the sharp plasmon structure in $W(\omega)$. This, in turn, will lead to a very broad satellite struc-

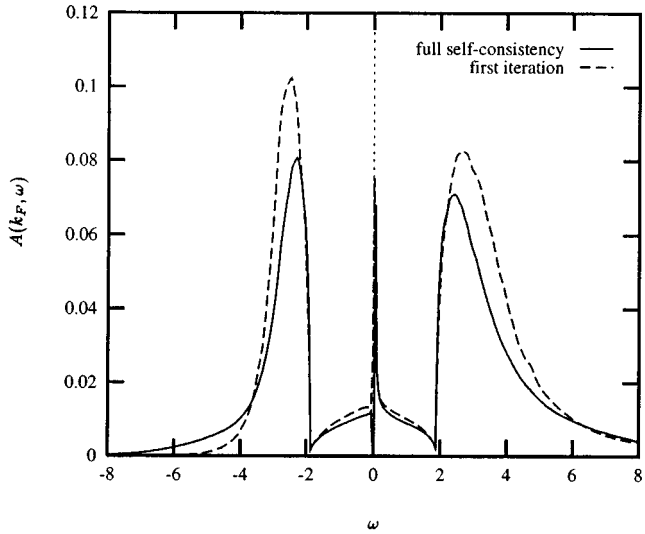

FIG. 9. The self-consistent spectral function $A(k=k_F,\omega)$ [Eq. (1)] compared to that of the first iteration. Here the quasiparticle peak is too large and narrow to be displayed in the figure. Only the plasmon side bands are shown ($r_s=4$).

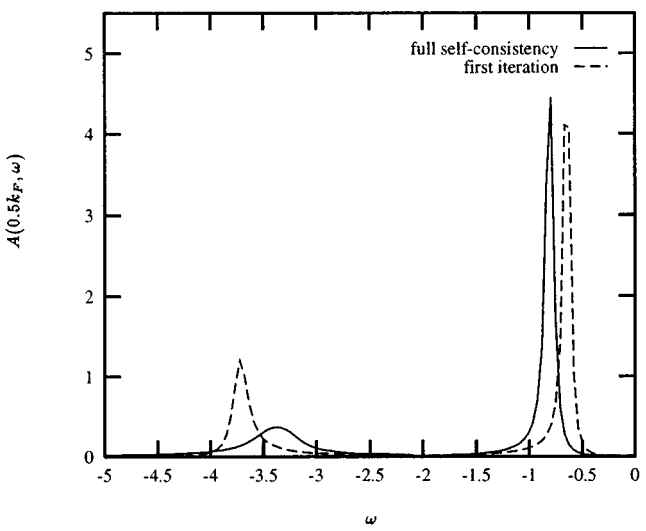

FIG. 10. The self-consistent spectral function $A(k=0.5k_F,\omega)$ [Eq. (1)] compared to that of the first iteration ($r_s=4$).

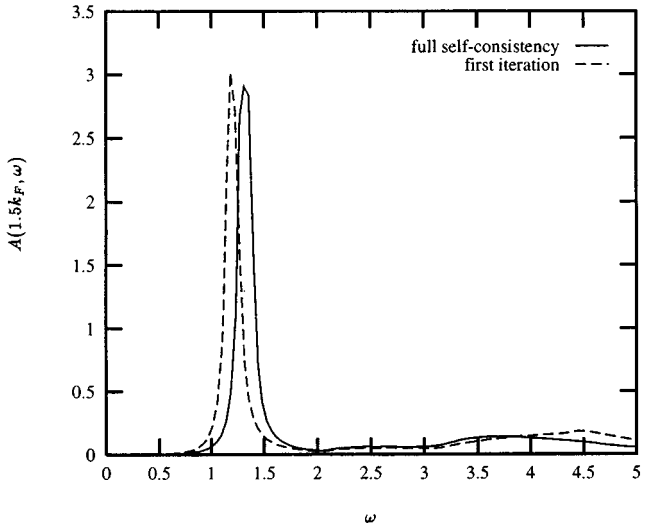

FIG. 11. The self-consistent spectral function $A(k=1.5k_F,\omega)$ [Eq. (1)] compared to that of the first iteration ($r_s=4$).

ture in the spectral function $A(\omega)$. The only conceivable self-consistent solution to the problem is a spectral function $A(\omega)$ with a relatively broad and diffuse structure around ω_p below the quasiparticle peak. Although such a result is in conflict with the experimental facts, we stress that there is nothing which would prevent the fully self-consistent theory from providing an accurate picture of the quasiparticles, including the total energy of the system. We are presently pursuing this very interesting problem.[18]

VI. CONCLUSIONS

We will here summarize our findings in a few sentences.

(1) Allowing the quasiparticles to broaden has a negligible effect on the final results.

(2) Allowing the quasiparticle energies to move from their free-electron positions has a very small effect on the final results for the electron gas.

(3) The main effects of self-consistency are caused by allowing for a reduction in the quasiparticle strength. Compared to ordinary *GW* results, i.e., the results of what in this work has been referred to as the first iteration, self-consistency leads to a smaller quasiparticle width, a substantially larger bandwidth, and a larger quasiparticle renormalization factor. All these effects are due to a smaller dynamical self-energy.

(4) The relatively bad description of the satellite structure due to plasmons in ordinary *GW* calculations is marginally improved.

(5) An attempt to include the screened potential in the self-consistency procedure is shown to lead to an even worse description of the satellite regions. However, nothing is yet known about full self-consistency with regard to quasiparticle properties. We hope to get back to this point in the near future.[18]

(6) Several of our results mentioned above demonstrate a strong need for vertex corrections even in such a simple system as the electron gas.

(7) A useful sum rum rule has been derived, which is valid in all *GW*-type calculations.

(8) Finally, we would like to stress that we have here demonstrated how physical insight can be used to obtain a decisive simplification of self-consistent calculations. The procedure is based on a representation of the Green function in terms of its spectral function, which, in turn, is represented as a sum of Gaussians.

ACKNOWLEDGMENTS

We thank the Eindhoven group with Professor W. van Haeringen and Dr. P. A. Bobbert and Dr. H. J. de Groot for stimulating discussion on the topic of self-consistent *GW* calculations. We also thank Professor L. Hedin for discussions on the *GW*A, and Professor C.-O. Almbladh for discussions on the fundamental aspects of many-body theory.

[1] M.S. Hybertsen and S.G. Louie, Phys. Rev. B **32**, 7005 (1985).
[2] M.S. Hybertsen and S.G. Louie, Phys. Rev. B **34**, 5390 (1986).
[3] R.W. Godby, M. Schluter, and L.J. Sham, Phys. Rev. B **37**, 10 159 (1988).
[4] F. Aryasetiawan, U. von Barth, P. Blaha, and K. Schwartz, Technical Report, Lund University, LU-TP 2/91, 1991.
[5] F. Aryasetiawan and U. von Barth, Phys. Scr. **T45**, 270 (1992).
[6] F. Aryasetiawan, Phys. Rev. B **46**, 13 051 (1992).
[7] F. Aryasetiawan and O. Gunnarsson, Phys. Rev. Lett. **74**, 3221 (1995).
[8] L. Hedin, Phys. Rev. **134**, A796 (1965).
[9] L. Hedin and S. Lundqvist, *Effects of Electron-Electron and Electron-Phonon Interactions on the One-Electron States of Solids*, edited by F. Seitz, D. Turnbull, and H. Ehrenreich, Solid

State Physics Vol. 23 (Academic, New York, 1969).
[10] H. J. de Groot, P. A. Bobbert, and W. van Haeringen, Phys. Rev. B **52**, 11 000 (1995).
[11] G. Baym and L.P. Kadanoff, Phys. Rev. **124**, 287 (1961).
[12] G. Baym, Phys. Rev. **127**, 1391 (1962).
[13] B. I. Lundqvist, Phys. Konden. Mater. **6**, 193 (1967).
[14] B. I. Lundqvist, Phys. Konden. Mater. **6**, 206 (1967).
[15] B. I. Lundqvist, Phys. Konden. Mater. **7**, 117 (1968).
[16] B. I. Lundqvist, Phys. Status Solidi **32**, 273 (1969).
[17] E. Jensen and E. W. Plummer, Phys. Rev. Lett. **55**, 1912 (1985).
[18] B. Holm and U. von Barth (unpublished).